AIP | Applied Physics Letters

Strain rate and adhesive energy dependent viscoplastic damage modeling for nanoparticulate composites: Molecular dynamics and micromechanical simulations

B. J. Yang, H. Shin, H. Kim, and H. K. Lee

Citation: Applied Physics Letters **104**, 101901 (2014); doi: 10.1063/1.4868034
View online: http://dx.doi.org/10.1063/1.4868034
View Table of Contents: http://scitation.aip.org/content/aip/journal/apl/104/10?ver=pdfcov
Published by the AIP Publishing

Strain rate and adhesive energy dependent viscoplastic damage modeling for nanoparticulate composites: Molecular dynamics and micromechanical simulations

B. J. Yang,[1] H. Shin,[2] H. Kim,[2] and H. K. Lee[1,a)]
[1]*Department of Civil and Environmental Engineering, Korea Advanced Institute of Science and Technology (KAIST), 291 Daehak-ro, Yuseong-gu, Daejeon 305-701, South Korea*
[2]*Graduate School of Energy Environment Water Sustainability (EEWS), Korea Advanced Institute of Science and Technology (KAIST), 291 Daehak-ro, Yuseong-gu, Daejeon 305-701, South Korea*

(Received 7 January 2014; accepted 26 February 2014; published online 10 March 2014)

A viscoplastic damage model based on molecular dynamics (MD) and micromechanics is proposed to predict the rate-dependent inelastic behavior of nanoparticle-reinforced polymer composites. The constitutive equation is developed by combining the solution of the elastic problem and Laplace-transformed superposition principle. The MD simulation is then conducted to derive the interfacial adhesive energy of nanocomposites (silica/nylon-6), and the MD results are applied to the viscoplastic damage model. Influences of the strain rate sensitivity and the interfacial debonding damage on nanocomposites are discussed, and predictions from the proposed approach are compared with experimental measurements to elucidate the potential of the formulation. © *2014 AIP Publishing LLC*. [http://dx.doi.org/10.1063/1.4868034]

Nanoparticulate composites, which are a mix of nanoparticles (NPs) and a polymer matrix, have been developed rapidly over the last decade due to their appealing mechanical properties.[1] Nanocomposites generally exhibit various improvements over conventional materials; however, the potential for the widespread use of nanocomposites is restricted owing to a lack of knowledge regarding the interfacial damage.[2,3] In addition, NP-reinforced composites are typically made of rigid NPs which exhibit elastic behavior, whereas the matrix generally shows viscoelastic and/or viscoplastic deformation, such as a polymer.[4] The inelastic behavior is induced by the viscous nature of the polymer, resulting in a rate-dependent property that significantly affects the overall behavior of polymer-based composites.[4] The variations in the interfacial damage and rate-dependent characteristics, which are considered as key issues pertaining to nanocomposites, must therefore be accounted for accurate predictions of the overall behavior of a nanocomposite system.[5,6]

Although numerous studies have been conducted to predict the mechanical behaviors of nanocomposite systems, relatively few have investigated the correlated behaviors among the rate-dependent viscoplasticity, the interfacial adhesive energy, and the debonding damage on the nanocomposites. Hence, the objective of this study is to develop a rigorous but effective multiscale constitutive model based on micromechanics and molecular dynamics (MD) simulations to analyze the overall viscoplastic behavior of nanoparticulate composites (silica/nylon-6) undergoing debonding damage. A separate derivation with the viscosity effect for the pre- and post-yield behavior is developed by means of micromechanics,[7,8] taking into account the damage mechanism and NP size. An atomistic MD simulation is then conducted directly to calculate the adhesive energy between NPs and the matrix, which is applied to the micromechanical frameworks.[9,10] The capability of the present model to predict the viscoplastic behavior of NP-reinforced composites is demonstrated through a number of experimental comparisons.

First, we assumed that the nanocomposites is composed of a viscoelastic polymer matrix (phase 0) and randomly located elastic NPs (phase 1).[11,12] With an increase in the external loading, interfacial debonding between NPs and a matrix may initiate once the local stresses at the interface reach a certain critical level,[13] and the debonded NPs are separately considered as phase 2. The damage mechanism is expressed as the current volume fraction of debonded NPs (ϕ_2), and they are estimated by Weibull probability model as follows:[14,15]

$$\phi_2 = \phi\left\{1 - \exp\left[-(\bar{\boldsymbol{\sigma}}_1/S_0)^M\right]\right\}, \tag{1}$$

where ϕ is the original volume fraction of NPs; S_0 and M are Weibull parameters which connect the fracture strength of NPs and the cracking evolution rate.[13] $\bar{\boldsymbol{\sigma}}_1$ is the internal stress of NP (phase 1), which can be calculated as[7,16]

$$\begin{aligned}\bar{\boldsymbol{\sigma}}_1 &= \begin{bmatrix}\mathbf{C}_1 \cdot \left\{\mathbf{I} - \mathbf{S}\cdot(\mathbf{A}_1 + \mathbf{S} - 1)^{-1}\right\}\cdot \\ \left\{\mathbf{I} - \sum_{q=1}^{2}\phi_q \mathbf{S}\cdot(\mathbf{A}_q + \mathbf{S})^{-1}\right\}\end{bmatrix} : \bar{\boldsymbol{\epsilon}} \\ &\equiv \left[U_1\delta_{ij}\delta_{kl} + U_2(\delta_{ik}\delta_{jl} + \delta_{il}\delta_{jk})\right] : \bar{\boldsymbol{\epsilon}},\end{aligned} \tag{2}$$

with

$$\mathbf{A}_q \equiv (\mathbf{C}_q - \mathbf{C}_0)^{-1}\cdot\mathbf{C}_0, \tag{3}$$

where $\mathbf{C}_q$ ($q = 0, 1, 2$) is elasticity tensor of q-phase and $\mathbf{I}$ is the fourth-order identity tensor. $\mathbf{S}$ is the Eshelby's tensor for a nano-inhomogeneity with the interface effect, which is given

a)Electronic mail: leeh@kaist.ac.kr

in Yang *et al.*[10] After a series of lengthy yet straightforward derivations, the parameters U_1 and U_2 can be determined, and they are given in the supplementary material.[17]

The Weibull parameter S_0 can be replaced with the critical debonding strength σ_{cri},[13] which is a material property that can be obtained either from direct experimental measurements or from an indirect method. The analytical solution for σ_{cri} at the interface region is considered in the present study, and the critical strength is expressed in terms of the adhesive energy[3,18]

$$\sigma_{cri} \cong \sqrt{(4\varphi E_0)/\{R(1+\nu_0)\}}, \tag{4}$$

where R is the radius of NP; E_0 and ν_0 are elastic modulus and Poisons's ratio of the matrix, respectively. φ is the adhesive energy at the interfacial region between the NPs and the matrix,[18] which can be calculated via MD simulations.

As a representative model, we consider the nylon-6 matrix system where silica (β-cristobalite) NPs are embedded as shown in Fig. 1(a). In order to identify the changes in adhesive energy with different constituents, seven different sets of nanocomposite system are considered. The Large-scale Atomistic Modeling Massively Parallelized Simulation (LAMMPS) code[19] is used for the MD simulations and DREIDING generic force field (FF)[20] is adopted to describe the interatomic potential. The full MD procedure to equilibrate the nanocomposite system is conducted as Yang *et al.*,[10] and details regarding the MD simulations and the FF validity are given in the Ref. 10. We note that the MD simulation procedure coupled with micromechanics was effective in predicting elastic properties of NP/nylon-6 composite materials.[11]

Based on the MD simulations, the adhesive energies (φ) of the silica NP/nylon-6 nanocomposites are evaluated as follows:[21]

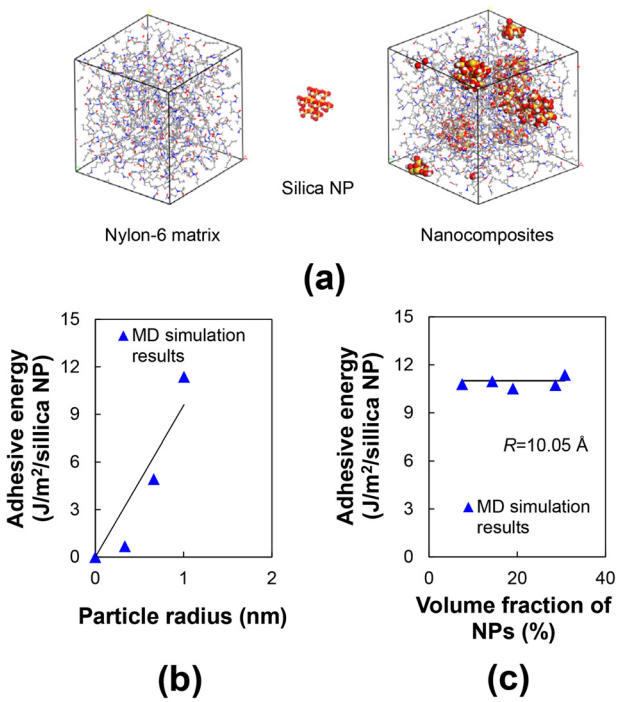

FIG. 1. (a) The representative structures of the material system, and the predicted adhesive energy between the silica NP and the matrix with varying (b) size and (c) volume fraction of NPs.

TABLE I Predicted adhesive energies with varying radius and volume fraction of the nanocomposite system obtained by MD simulations.

System	R (Å)	N_P	ϕ_1(%)	φ (J/m^2/silica)
w/SiO_4H_4	3.35	6	1.62	0.69
w/$Si_{17}O_{52}H_{36}$	6.62	6	11.28	4.93
w/$Si_{83}O_{220}H_{108}$	10.05	1	7.52	10.79
		2	14.34	10.97
		3	19.02	10.52
		5	28.64	10.74
		6	30.78	11.37

$$\varphi = \frac{\langle E_m \rangle + N_p E_p - \langle E_{NC} \rangle}{N_p}, \tag{5}$$

where $\langle E_m \rangle$ and $\langle E_{NC} \rangle$ mean the ensemble averaged MD potential energy of pure nylon matrix and nanocomposites, respectively, and E_p is the FF minimized energy of the silica NP. N_p denotes the number of silica NP in the simulation cell. The obtained adhesive energies are illustrated in Figs. 1(b) and 1(c) and summarized in Table I. It is shown in Fig. 1(b) that higher adhesive energies are observed as the radius of NP increases; however, the different volume fraction with same radius of NPs is insignificant on the adhesive energy of nanocomposites (Fig. 1(c)), noting that the adhesive energy is more influenced by NP size than volume fraction of the nanocomposites. Based on the present MD calculations, adhesive energy of silica/nylon-6 nanocomposites can be expressed as function of radius of NP as $\varphi = 9.56\ R$ J/m^2/silica.

The viscoelastic moduli can be derived based on the superposition principle of Laplace-transformation (LT) as follows:[8,22]

$$\begin{aligned}\left[\boldsymbol{\sigma} = \mathbf{C}_*^E : \boldsymbol{\epsilon}\right] &\rightarrow \left[\boldsymbol{\sigma}(s) = s\tilde{\mathbf{C}}_*(s) : \boldsymbol{\epsilon}(s)\right]^{\mathrm{LT}} \\ &\rightarrow \left[\sigma = \mathbf{C}_*^{VE} : \boldsymbol{\epsilon}\right]^{\text{Inverse LT}},\end{aligned} \tag{6}$$

where $\mathbf{C}_*^E$ is the effective elastic tensor of nanocomposites, s is the Laplace constant, and tilde ($\sim$) means the transformed domain (TD). Here, $\mathbf{C}_*^E$ can be determined by micromechanics-based method via[10]

$$\mathbf{C}_*^E = \mathbf{C}_0 \cdot \left[\mathbf{I} + \sum_{q=0}^{2} \left\{ \begin{array}{c} \phi_q(\mathbf{A}_q + \mathbf{S})^{-1} \cdot \\ \left[\mathbf{I} - \phi_q \mathbf{S} \cdot (\mathbf{A}_q + \mathbf{S})^{-1}\right]^{-1} \end{array} \right\}\right], \tag{7}$$

where ϕ_q is the volume fraction of q-phase. $\tilde{\mathbf{C}}_*(s)$ is made by replacing the elastic phase with the TD phase, as follows:[22]

$$\mu_0 \rightarrow \mu_0^{TD} = \frac{\eta_0 \mu_0 s}{\mu_0 + s\eta_0}, \quad \kappa_0 \rightarrow \kappa_0^{TD} = \frac{\eta_0 \kappa_0 s}{\mu_0 + s\eta_0}, \tag{8}$$

where μ_0, κ_0, and η_0 signify the shear, bulk modulus, and viscosity of the matrix, respectively. The effective viscoelastic constitutive equation $\mathbf{C}_*^{VE}$ can be then obtained by taking the direct inverse Laplace transform. A detailed aforementioned derivation process is given in the supplementary material,[17]

and the explicitly derived fourth-rank tensor $\mathbf{C}_*^{VE}$ is also listed in supplementary material.[17]

Moreover, the von-Mises J_2-yield criterion with an isotropic hardening law is adopted here to predict the overall viscoplastic behavior of nanocomposites. When a small deformation is considered, the total strain is as follows:[23]

$$\boldsymbol{\epsilon} = \boldsymbol{\epsilon}^{VE} + \boldsymbol{\epsilon}^{P}, \tag{9}$$

where $\boldsymbol{\epsilon}^{VE}$ and $\boldsymbol{\epsilon}^{P}$ are the overall viscoelastic and plastic strain, and the plastic strain $\boldsymbol{\epsilon}^{P}$ is occurred when the following yield function is satisfied[7,13]

$$\bar{F} = (1-\phi_1)\sqrt{\boldsymbol{\sigma} : \bar{\mathbf{T}} : \boldsymbol{\sigma}} - K(e^P) > 0, \tag{10}$$

with

$$K(e^p) = \sqrt{2/3}\left[\sigma_y + h(e^P)^q\right], \tag{11}$$

where the fourth-rank tensor $\bar{\mathbf{T}}$ is listed in supplementary material[16] and σ_y is the yield strength of the matrix. e^P represents the effective equivalent plastic strain, and h and q are plastic parameters.

The plastic parameters (h, q) are determined via a curve fitting with experimentally measured stress-strain responses of the matrix material. Hasan *et al.*[24] have investigated the uniaxial tensile behavior of the nylon-6 matrix under various strain rates ($\dot{\epsilon} = 2$, 0.2, and 0.02/min), and the experimental results are utilized for the comparison. The material properties adopted in the simulations are sourced from the experimental data:[24] $E_0 = 1.76$ GPa, $\nu_0 = 0.41$, $E_1 = 73.1$ GPa, $\nu_1 = 0.17$, $R = 20$ nm, $\phi_1 = 1\%$–2%, $\eta_0 = 200 \times \exp\{-2.1 \cdot \log(\dot{\epsilon})\}$ MPa · s, $\sigma_y = 64.4$ MPa at $\dot{\epsilon} = 0.02$ /min, 83.4 MPa at $\dot{\epsilon} = 0.2$ /min, and 125 MPa at $\dot{\epsilon} = 2$ /min.[24]

The fitted plastic parameters are $h = 170$ MPa and $q = 0.8$ at $\dot{\epsilon} = 2$/min, and the same estimated values for the parameters are applied to the $\dot{\epsilon} = 0.2$ and 0.02/min cases. It is observed from Fig. 2(a) that the present predictions match well with the experimental data for the matrix regardless the value of strain rates. Fig. 2(b) shows the elastic, viscoelastic, and viscoplastic stress-strain responses of nanocomposites under the uniaxial tensile loading. In order to illustrate the damage mechanism, the stress-strain predictions with and without the damage model are plotted in the same figure. As observed in Fig. 2(b), the elastic stress-strain responses exhibit much stiffer behavior compared to behaviors of the viscoelastic and viscoplastic cases. It is also observed that the viscoplastic prediction exhibits a sudden change from the viscoelastic to the viscoplastic deformation shortly after the yield point.

The viscoplastic stress-strain responses and the corresponding damage evolutions with different strain rates are shown in Figs. 3(a) and 3(b). They show that the strain rate affects the overall behavior of the composites, and the damage mechanism becomes more pronounced as the strain rate increases. As the debonding damage continues, the simulated viscoplastic stress-strain responses demonstrate a substantial departure from linearity.

The predicted viscoplastic responses of the silica NP-reinforced nylon-6 composites are compared with the

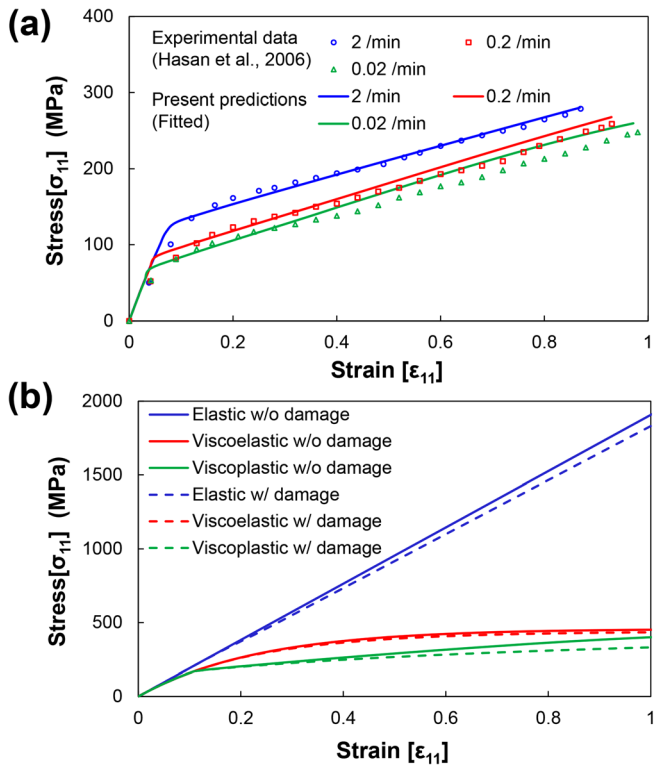

FIG. 2. (a) Comparisons between measured and fitted stress-strain curves of the nylon-6 matrix with varying strain rates and (b) the predictions of elastic, viscoelastic, and viscoplastic behavior of silica/nylon-6 nanocomposites with and without consideration of the damage phenomenon.

stress-strain curves experimentally obtained by Hasan *et al.*[24] The adopted model parameters are: $M = 7$ and $\varphi = 9.56R$ J/m^2/silica. It can be observed in Fig. 4(a) that the present predictions ($\phi_1 = 1\%$) which consider various strain rates match well with the experimental data in terms of the viscoelastic range and in the latter part of the plastic yielding range; a higher strain rate leads to a stiffer stress-strain behavior and a higher yield point. An experimental comparison with different NP volume fraction ($\phi_1 = 2\%$) are also conducted, showing that the predicted result of the nanocomposites is in good quantitative agreement with the experimental data.[24]

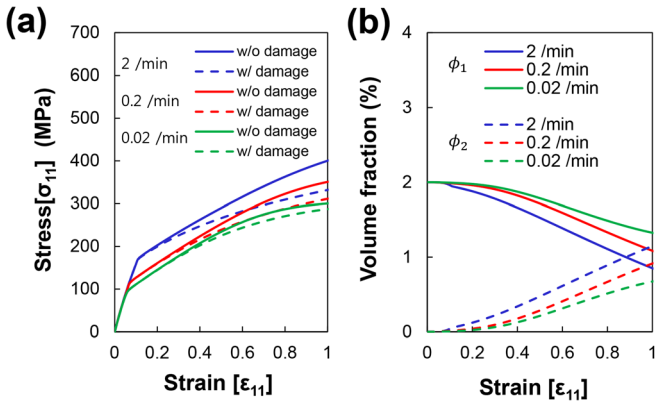

FIG. 3. (a) The viscoplastic stress-strain responses and (b) the corresponding damage evolutions of silica/nylon-6 nanocomposites with different values of strain rates.

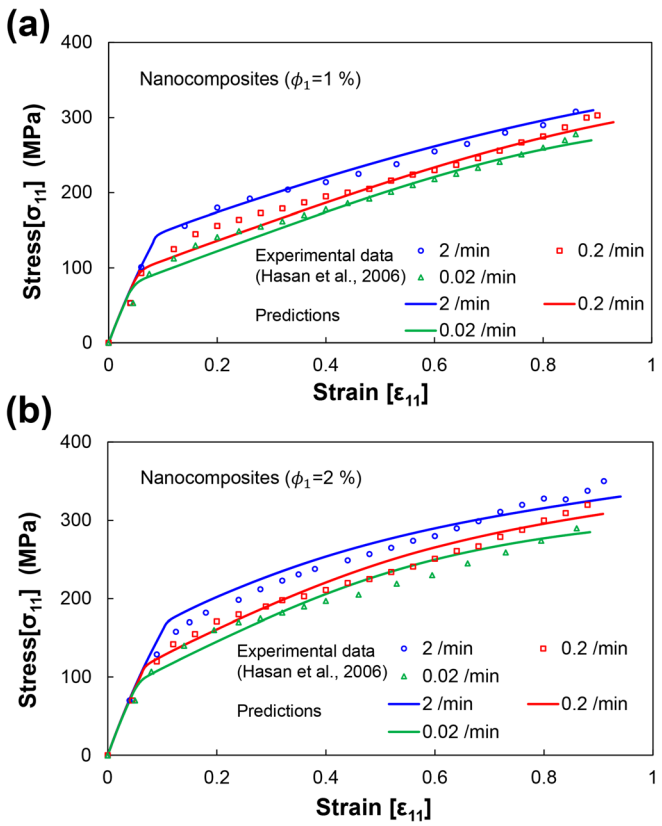

FIG. 4. Comparisons between the experimental data[24] and the present predictions for the nanocomposites containing (a) $\phi_1 = 1$ % and (b) $\phi_1 = 2$ % of NPs at different strain rates.

By accounting for the nature of NP debonding and strain rate sensitivity, a constitutive modeling framework to predict the viscoplastic damage behavior of nanoparticulate composites has been proposed.[25,26] The present formulation is based on the MD simulations and micromechanics, and the findings from a series of numerical simulations and experimental comparisons can be summarized as follows:

1. The adhesive energy depends on the particle size; a larger NP leads to higher adhesive energy. However, similar values of adhesive energy are calculated with different volume fractions of NPs, indicating the adhesive energy is not associated with the volume fraction of inclusions.
2. The higher value of the strain rate leads to a higher yield strength and stiffer stress-strain response; however, less damage mechanism is observed for nanocomposites with a decrease in the strain rate, whereas strong damage behavior is noted with a high level of strain rate.
3. Good agreement between the present predictions and experimental data shows the predictive capability of the proposed method.

This study has demonstrated the capability of the proposed micromechanical framework for predicting the viscoplastic damage behavior of NP-reinforced composites. We believe that the proposed method enables precise predictions of nanocomposites with various strain rate conditions. The constitutive model for nanoparticulate composites is, therefore, expected to be used to determine the volume concentration of the reinforcing NPs and plastic responses under different strain rate conditions.

This research was sponsored by the National Research Foundation of Korea (NRF) grants funded by the Korean government (2013028443 and 2012M1A2A2026588) and the National Institute of Supercomputing and Networking/Korea Institute of Science and Technology Information with supercomputing resources including technical support (KSC-2013-C3-019). H.S. and H.K. acknowledge the support by the Global Frontier R&D Program (2013-073298) on Center for Hybrid Interface Materials (HIM) funded by the Ministry of Science, ICT & Future Planning.

[1]B. R. Kim, S. H. Pyo, G. Lemaire, and H. K. Lee, Interact. Multiscale Mech. **4**, 173 (2011).
[2]H. K. Kim, I. W. Nam, and H. K. Lee, Compos. Struct. **107**, 60 (2014).
[3]M. Zappalorto, M. Salviato, and M. Quaresimin, Compos. Sci. Technol. **72**, 49 (2011).
[4]H. X. Li and C. P. Buckley, Int. J. Plasticity **26**, 1726 (2010).
[5]J. L. Le and Z. P. Bazant, J. Mech. Phys. Solids **59**, 1291 (2011).
[6]R. Tawie, H. K. Lee, and S. H. Park, Smart Struct. Syst. **6**, 851 (2010).
[7]J. W. Ju and H. K. Lee, Int. J. Solids Struct. **38**, 6307 (2001).
[8]B. J. Yang, B. R. Kim, and H. K. Lee, Acta. Mech. **223**, 1307 (2012).
[9]H. Shin, T. A. Pascal, W. A. Goddard, and H. Kim, J. Phys. Chem. B **117**, 916 (2013).
[10]B. J. Yang, H. Shin, H. K. Lee, and H. Kim, Appl. Phys. Lett. **103**, 241903 (2013).
[11]Z. Liang, H. K. Lee, and W. Suaris, Int. J. Solids Struct. **43**, 5674 (2006).
[12]H. K. Lee and S. H. Pyo, Int. J. Solids Struct. **45**, 1614 (2008).
[13]L. Z. Sun, H. T. Liu, and J. W. Ju, Int. J. Numer. Methods Eng. **56**, 2183 (2003).
[14]H. K. Lee and S. H. Pyo, Int. J. Solids. Struct. **44**, 8390 (2007).
[15]H. K. Lee, S. Simunovic, and D. K. Shin, Comput. Mater. Sci. **29**, 459 (2004).
[16]H. K. Lee and S. H. Pyo, Compos. Sci. Technol. **68**, 387 (2008).
[17]See supplementary material at http://dx.doi.org/10.1063/1.4868034 for the process and results of the present simulations.
[18]J. Chen, G. Weng, Z. Yu, Z. Huang, and Y. Mai, Compos. Sci. Technol. **70**, 861 (2010).
[19]S. Plimpton, J. Comput. Phys. **117**, 1 (1995).
[20]S. L. Mayo, B. D. Olafson, and W. A. Goddard, J. Phys. Chem. **94**, 8897 (1990).
[21]J. Tersoff, Phys. Rev. B **37**, 6991 (1988).
[22]J. Li and G. J. Weng, J. Eng. Mater. Technol. **116**, 495 (1994).
[23]S. H. Pyo and H. K. Lee, Int. J. Plasticity **26**, 25 (2010).
[24]M. M. Hasan, Y. Zhou, H. Mahfuz, and S. Jeelani, Mater. Sci. Eng. A **429**, 181 (2006).
[25]H. K. Lee and S. Simunovic, Compos. Part B-Eng. **31**, 77 (2000).
[26]H. K. Lee and S. Simunovic, Int. J. Solids Struct. **38**, 875 (2001).